



Modelling of Sonic Boom Phenomena

Tatiana A. Kiseleva¹, Aleksandr D. Kosinov², Yurii G. Ermolaev³, Vladislav F. Volkov⁴

Abstract

To create a supersonic airplane with low sonic boom, we must develop the physical modeling of this phenomenon. This paper proposes improvement on the experimental method for studies of the airplane near-field. The method based on for simultaneous measurement of pressure and average mass flow rate in the dynamic recording mode in the conditions of the T-313 wind tunnel of the Institute of Theoretical and Applied Mechanics Siberian Branch of the Russian Academy of Sciences. It is shown that the correlation of the average mass flow with the pressure distributions is observed.

Keywords: *supersonic business jet, sonic boom, research methods, thermoanemometer*

1. Introduction

The creation of a supersonic second-generation passenger aircraft will be a significant evolution in the development and use of airspace. Traveling about two to three times faster than civil aircraft currently in operation, a supersonic passenger aircraft is able to radically change the available concept of an air travel. However, with the rapid development of military supersonic aviation, the second-generation supersonic passenger aircraft is still not created. Along with the high energy consumption, the sonic boom (SB) by a heavy aircraft during a flight at supersonic speed remains an acute problem [1]. The disturbed flow during the motion of the aircraft with supersonic speed contains the head shock wave (SW) from the nose of the aircraft, and the tail SW formed in the aft part.

Near the aircraft flying with the supersonic velocity, there are intermediate SW, plus rarefaction and compression waves created by individual elements of the aircraft. As non-linear effects (speed of disturbance propagation versus the disturbance amplitude) propagate in the atmosphere, the flow pattern transforms in the N-profile of the disturbed pressure wave which is referred to as the "N-wave" of the sonic boom. Suddenness and short duration of the N-wave action are perceived negatively by humans and alive creatures. People undergoing periodical action of the sonic boom may suffer from psychological and physiological diseases; animals may change the habitat, etc. Today, the supersonic overland missions are prohibited both in the USA and Europe. In Russia, the pressure drop at the SB wave of $90 \text{ Pa} \pm 20 \text{ Pa}$ was introduced in the State Standard (GOST) 23552-79 1979 as an optional value. Note that, during the cruise-altitude flights of Tu-144, the level sonic boom correlated to the prescribed value. Nowadays, the International Civil Aircraft Organization (ICAO) is developing the standards for the sonic boom level acceptable for humans.

¹ *Novosibirsk State University, Pirogova str. 2, Novosibirsk, 630090, Russia
Khristianovich Institute of Theoretical and Applied Mechanics, Siberian Branch of Russian Academy of Sciences,
Institutskaya str. 4/1, Novosibirsk, 630090, Russian Federation, bobarykina@ngs.ru*

² *Novosibirsk State University, Pirogova str. 2, Novosibirsk, 630090, Russia
Khristianovich Institute of Theoretical and Applied Mechanics, Siberian Branch of Russian Academy of Sciences,
Institutskaya str. 4/1, Novosibirsk, 630090, Russian Federation, kosinov@itam.nsc.ru*

³ *Novosibirsk State University, Pirogova str. 2, Novosibirsk, 630090, Russia
Khristianovich Institute of Theoretical and Applied Mechanics, Siberian Branch of Russian Academy of Sciences,
Institutskaya str. 4/1, Novosibirsk, 630090, Russian Federation, yermol@itam.nsc.ru*

⁴ *Khristianovich Institute of Theoretical and Applied Mechanics, Siberian Branch of Russian Academy of Sciences,
Institutskaya str. 4/1, Novosibirsk, 630090, Russian Federation, volkov@itam.nsc.ru*

The aircraft SB level depends on the aircraft shape, size, real atmosphere conditions, local relief, etc. Contradictory requirements to the configuration make it difficult to create an environmentally friendly aircraft with the acceptable sonic boom level which would have the high aerodynamic quality and hence the marketability. This is especially important for heavy aircrafts (above 1000 kN), which is caused by the increased contribution of the lifting force in the sonic boom rising along with the aircraft weight. Today, intensive research is focused both on the conventional (passive) ways of protection from the SB based on the varying aircraft shape, and active methods of the direct action on the flow around the aircraft [2].

2. Modelling of the sonic boom phenomenon

The main problem of SB modelling is the large extent of the area under investigation, where the perturbed pressure levels vary by several orders of magnitude.

Normally, the sonic boom phenomenon is studied in the near and far fields. The near field of the SB adjoins the aircraft and has a complicated flow structure with shock waves, rarefaction and compression waves; its length is about the aircraft length ($K = H/L \sim L$, where H is the height distance from the aircraft, L is its characteristic size). The length of the far field where the sonic boom parameters vary feasibly in accordance with the asymptotic law, realizes within the distances of $K \sim L^2$. The middle zone of the SB is an intermediate one between the near and far fields and features the presence of intermediate shock waves on the pressure profile of the sonic boom wave; these waves are generated by the main elements of the aircraft configuration, for example, from a wing or nacelles.

There are various approaches to the study of the SB phenomenon:

- Flight (full-scale) tests;
- Experimental simulation of the SB phenomenon in aeroballistic installations, in wind tunnels of short-term or periodic action;
- Calculation methods;

Flight tests are the most informative and reliable, but extremely complex and expensive. Numerical modelling is the main research method, but it requires huge computational capability, the construction of complex grids to describe aircraft configurations, and, in addition, contains some assumptions. In this context, the numerical modelling of the sonic boom phenomenon should be added by experimental investigations purposed to obtain reliable information for the bodies of arbitrary configuration, and to validate the results of numerical calculations. Wind tunnels are commonly used to perform the physical simulation of the sonic boom wave formation and propagation; with the aid of wind tunnels, the fundamental task of the interaction, propagation, and methods of diagnostics of weak shock waves in the near field of the flow can be considered.

In ITAM SB RAS, under the supervision of Academician V. V. Struminskij, the combined experimental and computational approach has been developed to model the sonic boom effect [3]. The experimental part of the method is based on the modelling of the near field of the sonic boom in small-size wind tunnels with large models. Evolution of the measured distributions of the disturbed pressure propagating over long distances is determined by the computational methods based on the quasi-linear theory [4].

The major information obtained experimentally about the SB wave is the spatial distribution of the disturbed pressure generated by the aircraft. The intensity of the head SW and the pressure disturbed behind decreases essentially while distancing from the model. Normally, the parameters of the disturbed flow are detected discretely in each point by the pneumo-metric method with different pressure tubes involved [5]. Among them, there is an axisymmetric probe of static pressure, stagnation pressure tube (the Pitot tube), and the static pressure probe shaped as a plate with one receiving hole on the surface installed along with the flow. To measure the full pressure profile behind the reflected SW within one reading, the drained measurement plate is used [6], or the measurement surfaces covered with luminescent pressure transmitters [7]. In every case, the interaction between the studied SW and measurement probe results in additive systematic measurement errors. These errors depend on the measurement probe type and are highly sensitive to the flow Mach number and intensity of the studied shock waves.

As an improvement on the original method we propose a method for measuring the SB parameters in the near-field with the help of a hot-wire anemometer, used as a rule to measure the average and pulsating flow parameters in a supersonic boundary layer [8]. Low inertia, high sensitivity and compactness of the hot-wire anemometer sensor allow practically eliminating the errors associated with the interaction of the sensor with the investigated flow, as well as ensuring high reliability of measurements at high resolution in space.

The work is purposed to develop and approbation of the technique of experimental investigation of the near field by the pneumometric and hot-wire anemometric methods in order to reduce the sonic boom of supersonic aircrafts.

3. Experimental apparatus and procedure

3.1. Experimental methods

Fig. 1 shows the experiment schematic. The investigations were carried out in the wind tunnel T-313 (analogue of T-113 TsAGI) on the following modes: Mach number $M = 2.04$, unit Reynolds number of the incoming flow $Re_1 = (15-25) \cdot 10^6$, total temperature $T_0 = 283$ K. The dimensions of the rectangular section of the working part were $0.6 \times 0.6 \times 2$ m.

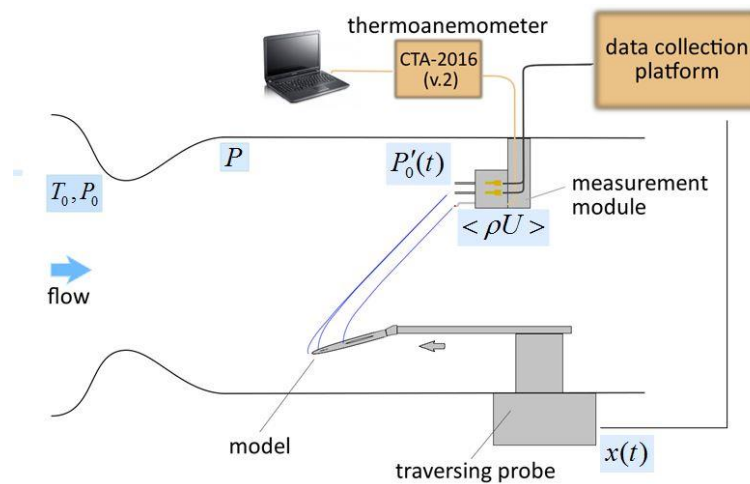


Fig 1. Experimental scheme

The experimental equipment includes: a model coordinator, a model, measuring probes, and the standard measuring complex of the wind tunnel T-313.

Recorded during the experiment parameters and the corresponding sensors are listed in the Table 1.

Table 1. Measured parameters and corresponding gage numbers

Gage number	Parameter	Unit
D1	P_0'	Pa
D2	P_0'	Pa
D3	x	mm
D4	P	Pa
D5	T_0	K
D6	P_0	Pa
D7	ρU	Kg/m ² s

The model coordinator is installed on the bottom wall of the working part in the wind tunnel. On the coordinator driver shaft there is a sensor of model motion along the lengthwise coordinate D3(X) (Fig. 1). On the upper wall of the working part there is a pylon on which the removable measurement unit

is fastened; in this unit there are the measurement probes of full pressure behind the normal shock wave (the Pitot tubes), and the hot-wire anemometer (see Fig. 2).

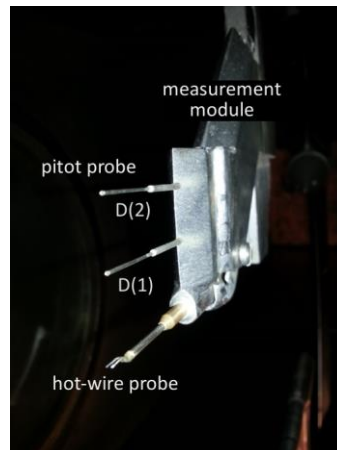


Fig 2. Photo of the measuring module in the working part of T-313

Strain pressure gages D1, D2, type TDM-A-0,16 with the rated pressure of 0.16 MPa were used in the experiments. The calibration tests showed that the maximum deviation did not exceed 6 Pa.

Measured signals through the automated switching system HP34970A entered the 45-channel recording multimeter, registering 5.5 decimal places with an error of 0.004%, followed by the transfer of digital information to the PC for writing to the database and subsequent processing.

During the experiment, the model fastened with the aid of a tail holder on the model coordinator, was permanently moved with the assigned speed in the lengthwise direction windward the freestream in respect to the immovable measurement probe. During this process, the discrete readings of six gages (D1 – D6) were registered with the assigned time step (about 400 ms) or coordinate pitch (about 0.5 mm at the movement speed of 1.3 mm/s)). The profile of the disturbed static pressure is detected from the arrays of the measured values from three gages (D2 (or D1), D3, D4), which after the primary processing correspond to: the absolute disturbed pressures behind the normal shock wave – the gage D2 or D1, the absolute full pressure of the flow – the gage D4, and the lengthwise coordinates at which the readings are counted – the gage D3.

Due to the low intensity of the studied SW, the free stream static pressure and Mach number were determined under the assumption of the flow isentropicity, involving the known relations of the gas-dynamic parameters in the flow point:

$$\frac{P}{P_0} = \left(1 + \frac{\gamma-1}{2} M^2\right)^{\frac{-\gamma}{\gamma-1}} \quad (1)$$

$$\frac{P_0^I}{P_0} = \frac{(\gamma+1)^{\frac{\gamma+1}{\gamma-1}}}{2} \cdot \frac{M^{\frac{2\gamma}{\gamma-1}}}{\left(1 + \frac{\gamma-1}{2} M^2\right)^{\frac{\gamma}{\gamma-1}} \left(\gamma M^2 - \frac{\gamma-1}{2}\right)^{\frac{1}{\gamma-1}}} \quad (2)$$

The solution of the Eq. 2 for the certain time instant t in the i -point of the flow at the values of P_{0i}^I and P_{0i} known from the experiment (they correlate to the pressure measured by the gages D1 and D4 (or D2 and D4)), dictates the Mach number value M_i . Taking into account that the full pressure of the flow varies during the experiment much slower than the pressure equalizes in the pneumatic channel of the gage D4, as well as the fact that slight variations of the full pressure (because of the instability of the assigned mode) impose almost no effect on the varying Mach number due to viscous effects, one can take that the average Mach number has been detected with the acceptable accuracy. The relative excessive static pressure is determined as:

$$\overline{\Delta P} = \frac{P_i}{P_\infty} - 1 \quad (3)$$

Note that the measurements of the pressure in one flow point, plus the measures to reduce the effect of the flow nonuniformity permit increasing essentially the measurement accuracy.

The following equipment was used to measure the average mass flow in the near field of the model:

- Hot-wire anemometer CTA-2016 (v.2);
- Digital oscilloscope Tektronix 1012b;
- PC;

Prior to the experiments, the cold resistance of the hot-wire anemometer wire was measured, and the overheating resistance was found. Then the frequency response of the hot-wire anemometer was adjusted with the aid of the test signal incorporated in the hot-wire anemometer. To adjust the hot-wire anemometer, the two-channel digital oscilloscope Tektronix 1012b was used. After the adjustment, the oscilloscope was cut off, and the measurements were carried out with the AD converter in the hot-wire anemometer. The measurement results were recorded by the PC connected with the hot-wire anemometer through the COM-port.

The sensitive element of the hot-wire anemometer is a tungsten wire (diameter 10 micrometres) or a molybdenum wire (diameter 40 micrometres) welded onto sharpened ends of steel currents ducts of the anemometer.

3.2. The model

The investigations were carried out with the model shaped as a tandem of two wings on the fuselage. The general view of the model is shown in Fig. 3.



Fig 3. Photo of the model

The fuselage length is $L = 140$ mm, its maximal diameter corresponding to the cylindrical parts is $d_m = 10.7$ mm. The canard wing geometrically similar to the main one was installed within the distance of the side chord start from the fuselage nose of 27.5 mm. The area of the canard wing was 10% of the total wings area.

The model was fixed on the coordinator shaft under the angle of attach of 3.5° . The true angle of attack of the model in the supersonic flow might reach $\alpha = 5^\circ$, the holder deformation from the transversal loading is taken into account.

4. Results and discussion

Fig. 4 presents the results of measurement of the full pressure profiles behind the normal shock waves generated by the model. During the initial motion of the model in respect to the measurement probes, the effect of the head SW on the probe readings was excluded. These data were taken as the full pressure behind the normal shock wave in the undisturbed flow $P_0'_{\infty}$. The relative excessive full pressure behind the normal shock wave was rated on the value $P_0'_{\infty}$ averaged by several points:

$$\overline{\Delta P_0'} = \frac{P_0'}{P_0'_{\infty}} - 1 \quad (4)$$

Every linear value is referred to the fuselage length L , i.e. are presented in calibers: $K = H/L$ is the relative distancing (transversal) of the model from the measurement probe, $\bar{x} = x/L$ is the relative lengthwise coordinate of the disturbed parameters profile.

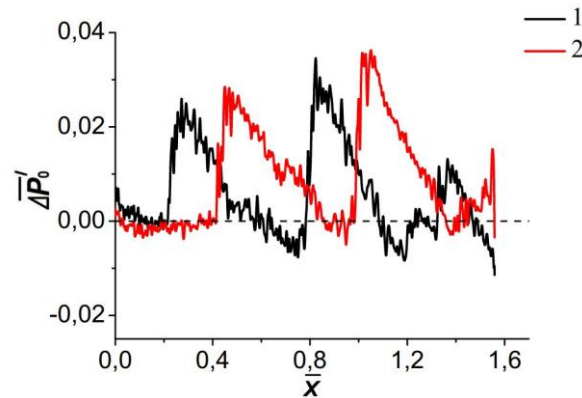


Fig 4. The full pressure behind a direct shock wave (Pitot pressure) profiles as a function of the coordinate: 1 - at a distance from the model nose $K = 1.43$ (D1), 2 - $K = 1.54$ (D2)

The coordinate beginning ($x = 0$ mm) corresponds to the initial point of the model motion. The pressure profiles measured by the pressure gage D1 correlate to the distance $K = H/L = 1.43$ (1), the pressure gage D2 – $K = 1.54$ (2), the hot-wire anemometer - $K = 1.28$, where H is the distance from the model nose to the measurement probe, $L = 140$ mm is the model length.

The profiles include: the head and intermediate shock waves and the compression wave formed by the shock waves from the fuselage nose, wing, and expanding part of the model holder, respectively.

Fig. 5. shows the profiles in respect to the excessive static pressure versus the relative coordinate calculated from the initial data in the ratios (1)-(2).

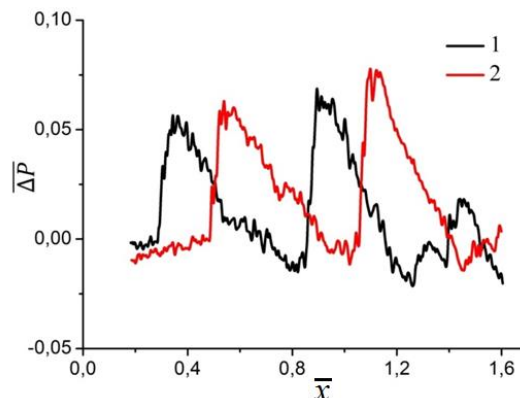


Fig 5. The relative excess static pressure as a function of normalized coordinate: 1 - at a distance from the model nose $K = 1.43$ (D1), 2 - $K = 1.54$ (D2)

Because of the complexity of the experiments with the hot-wire anemometers in T-313 and high probability of the breach of the wire in the hot-wire anemometer, it is necessary to minimize the experiment time. For this purpose, the initial model position is based on the need to minimize the time of measurement of the undisturbed flow parameters, which are measured before the head SW comes from the model into the coordinate x corresponding to the hot-wire anemometer position. With the assigned model position, the head SW came from the model directly on the sensor of the hot-wire anemometer prior to the model motion. Fig. 6 demonstrates the mass flow rate distribution in the near field of the model versus the mass flow rate of the undisturbed flow with due regard to the above described peculiarities of the experiment procedure. The parameters of the undisturbed flow and head shock wave front were not registered in the distribution of the average mass flow rate.

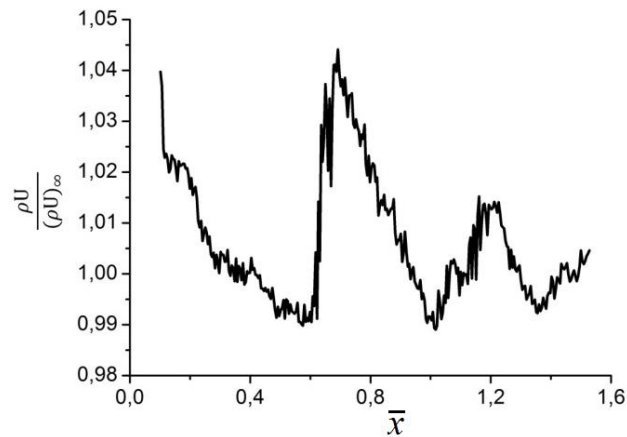


Fig 6. The profiles of the average mass flow rate at a distance from the model nose $K = 1.28$

The signals from the sensors of the measurement system of T-313 were not synchronized with the readings of the hot-wire anemometer sensor. The data were synchronized by comparing the data from the hot-wire anemometer and the information obtained from the measurement of the full pressure behind the normal shock wave during this experiment by the gages D1 and D2 included in the measurement system T-313. Comparison of the main elements of the flow from the distributions of the full pressure behind the normal shock wave and mass flow rate, and the time shift of the latter by Δt , enabled to find the position of the head shock wave from the model for the profile of the average mass flow rate (Fig. 7). It is evident from Fig. 7 that there is the qualitative agreement between the data obtained by the hot-wire anemometric and pneumometric methods.

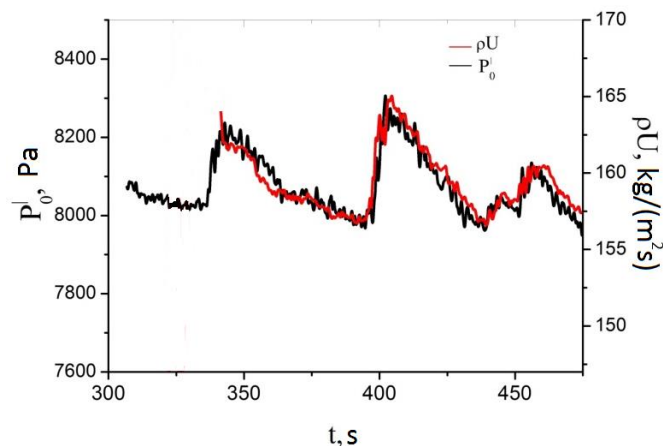


Fig 7. Hot-wire anemometric and pneumometric measurements comparison

5. Conclusions

To validate the results of the numerical modelling of the sonic boom phenomenon, it is necessary to perform experimental investigations in order to have the reliable experimental information about the flow parameters near the bodies of arbitrary configuration. Physical modelling of the processes of formation and propagation of the shock waves in the near field of the sonic boom is carried out in wind tunnels. Available techniques allow using the experimental data obtained in the near field of the sonic boom for the far field.

To increase the capability of the experimental investigations and gather additive information about the sonic boom wave, the method of simultaneous measurement of the pressure and mass flow rate in the dynamic mode of model near field registration has been vindicated and applied in the wind tunnel T-313; the method was realized as the automated measurement system.

The technique of measuring pressure profiles and mean mass flow rate in the near field of the model is described.

The application of the technique for obtaining the pressure distribution and the average mass flow rate, under the conditions of the T-313 wind tunnel, is demonstrated. It is shown that the correlation of the average mass flow with the pressure distributions is observed.

References

1. Chernyshev, S. L.: Sonic boom. Nauka Publishing, Moscow (2011)
2. Kiseleva, T.A., Golyshev, A.A., Yakovlev, V.I., Orishich, A.M.: The influence of the thermal wake due to pulsating optical discharge on the aerodynamic-drag force. *Thermophys. Aeromech.* (2018). <https://www.doi.org/10.1134/S0869864318020117>
3. Chirkashenko, V. F., Yudinzev, Yu. N.: Development of a technique for the measurement of the parameters of sonic shock in supersonic wind tunnels. Preprint № 6–83, *Izd. Inst. Theor. Prikl. Mekh.*, Novosibirsk (1983)
4. Whitham, G. B.: The flow pattern of a supersonic projectile. *Comm. Pure Appl. Math.* 5, 301–338 (1952)
5. Petunin, A.N.. *Methods and techniques for measuring gas flow parameters.* Mechanical Engineering, Moscow (1996)
6. Fomin, V.M., Chirkashenko, V.F., Volkov, V.F. et al.: Reduction of the sonic boom level in supersonic aircraft flight by the method of surface cooling. *Thermophys. Aeromech.* (2013) <https://doi.org/10.1134/S0869864313060036>
7. Mosharov, V.E.: Luminescent methods for investigating surface gas flows. *Instrum. Exp. Tech.* (2009) <https://doi.org/10.1134/S0020441209010011>
8. Vaganov, A.V., Ermolaev, Y.G., Kolosov, G.L. et al.: Impact of incident Mach wave on supersonic boundary layer. *Thermophys. Aeromech.* (2016). <https://doi.org/10.1134/S0869864316010054>